Conjugate effect of ionospheric heating observed by HINOTORI satellite

Yoshihiro Kakinami[1], Koh-Ichiro Oyama[1], Jann-Yenq Liu[1]
[1]Institute of Space Science, National Central University, Taiwan

Abstract

We investigated onset time of ionospheric heating and heating rate of electron temperature caused by the conjugate photoelectrons in low- and mid-latitude observed by HINOTORI satellite which observed electron temperature and density about 600 km altitude. Data which was obtained during Kp < 4 and Dst > -50 was used. We calculated the onset time map of low- and mid-latitude and found that the onset times vary with the magnetic field line length and intensity of F10.7. The onset time becomes constant, which is 10 minutes ahead of sunrise at 100 km, when the magnetic field line length is shorter than 5000 km. The onset time becomes early as F10.7 increase in this case. On the other hand, the onset time delay as the magnetic field line length increases when the magnetic field line length is over 5000 km. The heating rates of electron temperature decrease with increase of length of the magnetic field line when the magnetic field line length is shorter than 5000 km and almost constant when the magnetic field line length is over 5000 km. Our results suggest that flux of photoelectron escaping from sunlit ionosphere decrease during traveling to predawn ionosphere.

Introduction

Photoelectron produced by solar EUV can escape into outer ionosphere above 300 km altitude along the magnetic field line, where mean free path is comparable in scale height and reach conjugate ionosphere [Mariani, 1964]. Many author have been studied phenomena caused by conjugate photoelectron since 1960s. One of the phenomenon which are arised from the conjugate photoelectrons is predawn enhancement of 630 nm airglow [Barbier, 1961; Cole, 1965]. The onset of the airglow occurs 70 minutes at solar maximum earlier than at solar minimum [Carlson and Weill, 1967]. Cole [1965] suggested that the conjugate photoelectrons would lead temperatures of ambient electron high enough to account for the predawn enhancement of 630 nm emissions through thermal electron excitation, but observed electron temperature (Te) is not enough to explain the emission. Nagy and Banks [1970] proposed from their theoretical calculation that direct excitation of O atoms by the incoming photoelectrons cause predawn enhancement of the airglow. Direct measurements of the photoelectrons arriving from sunlit ionosphere were obtained at 1000

km altitude by Explorer 31 [Rao and Donley, 1969]. The photoelectrons from sunlit ionosphere around 300 km altitude and predawn airglow were observed simultaneously by rocket experiment [Sheperd et al., 1978]. More than 65 % of the emission could be produced by direct excitation.

Another phenomenon caused by the conjugate photoelectrons is predawn Te enhancement. The predawn Te enhancement has also been observed over Arecibo (18.4 N, 66.9 W) by using incoherent backscatter spectrum [Carlson, 1966]. Onset time of ionospheric heating corresponds to sunrise time about 100 km of conjugate point. Similar predawn Te enhancement observed over Millstone Hill (42.5 N, 71.5 W) [Evans, 1967b] and over Saint Santin (44.6 N, 2.2 E) [Bauer and Petit, 1970]. The onset of ionospheric heating has been observed when magnetic conjugate point reaches between 98 and 99 degrees in solar zenith angle (SZA) even in local night [Carlson and Weill, 1967].

Photoelectrons loss their energy not only through collisions with neutral particles at lower altitude but also through elastic collisions with ambient electron at altitudes of 1000 km and above. These energy losses contribute to heating of plasmasphere electrons [Mantas et al., 1978]. The heating has been observed around 1200 km altitude [Carlson, 1968]. Balan et al. [1996] suggested that 50 % of total energy of trapping photoelectrons contribute as heat source of plasmasphere. Conjugate photoelectron effect has been investigated by many authors. However, most of the reports of conjugate photoelectron effect were solely based on the ground observation and in higher latitude such as Arecibo [Carlson, 1966] so far. Therefore effects of photoelectron arriving from sunlit ionosphere still have not been adequately investigated. Spatial distribution of the onset time of ionospheric heating and heating rate in predawn ionosphere has been still unknown.

Similar situation of predawn occur during solar eclipse event. Local photoelectron production reduces in solar eclipse region, but conjugate point is still sunlit. Te enhanced about 500 K at 1000 km altitude compared to the case that conjugate photoelectron heating was neglected [MacPherson, et al., 2000]. This fact suggests that conjugate photoelectron heating plays an important role during solar eclipse event.

Recently, Chao et al. [2003] found characteristic ion temperature (Ti) enhancement observed by ROCSAT-1/IPEI instrument in June and December solstice. They pointed out that the predawn Ti enhancement is caused by photoelectron heating arriving from conjugate point.

A sun observation satellite, HINOTORI, which was put into a circular orbit of about 600 km with an inclination of 31 degrees, had two unique plasma probes. One of them is an electron temperature probe [Oyama, 1994] and the other is an impedance probe [Oya et al., 1986]. Observations of HINOTORI satellite have improved our understanding in mid- and

low-latitude ionosphere at 600 km altitude. Electron temperature in plasma bubble was studied systematically [Oyama et al., 1988].

In this paper, we attempt to investigate the onset time of ionospheric heating and heating rate associated with photoelectrons from conjugate ionosphere by using data of HINOTORI satellite.

Data set and results

HINOTORI satellite observed Te from February 1981 to June 1982 with 10 seconds time resolution about 600 km altitude. Absolute accuracy of Te is within 50 K [Oyama, 1994]. In low- and mid-latitude at 600 km altitude, Figure 1 shows local time (LT) variations of Te (top) with respect to the satellite location of latitude (middle) and longitude (bottom) in June solstice, respectively. Te takes the minimum value around 4 LT, rises steeply and shows a first peak around 7 LT, which is called morning overshoot. After the morning overshoot, Te reduces toward noon with increasing Ne, increase again around 15 LT, and shows the second peak, which is called afternoon overshoot, around 17 LT. Te decreases again toward morning [Oyama et al, 1996]. Orbits of HINOTORI satellite in Figure 1 were almost the same in latitude but different in longitude, that is, local sunrise time was almost the same. Onset time of ionospheric heating, which Te starts to rise, was observed at 4.67 LT in orbit 6533 (24.2S, 44.7W). On the other hand, the observed onset times were at 4.56 LT in orbit 6531 (25.1S 2.0W) and at 4.49 LT in orbit 6530 (25.6S 25.0E), respectively. Figure 1 shows longitudinal variation of the observed onset time. Heating rate of Te become steep as the observed onset time is late.

The onset of ionospheric heating observed in Arecibo coincided with SZA of 98-99 degrees in solar minimum [Carlson and Weill, 1967]. This range of SZA corresponds to predawn sunrise time at 62.7-79.5 km altitude. Another ground based observation showed the onset of ionospheric heating occurred when the conjugate sunrise at 100 km altitude [Carlson, 1966]. This is consistent with theoretical consideration with optical depth of EUV [Swider, 1964]. The onset has been observed at SZA of 102 degrees, which is equivalent to the sunrise time at 142.5 km altitude, in high solar activity [Carlson, 1968]. Evans [1967a] reported the onset of heating occurred at 100-106 degree. In this paper, therefore we defined sunrise at 100 km altitude as ionospheric sunrise.

Figure 2 shows distributions of ionospheric sunrise time at 100 km projected to satellite height (600 km) along the magnetic field line. The sunrise time at 100 km altitude in March (Figure 2a) are similar to that in September equinox (Figure 2c), but averaged onset time in September is about 30 minutes earlier than that in March. Two early sunrise regions exist around -20 degrees in latitude and 200 degree in longitude and around 20 degrees in

latitude and 320 degrees in longitude. Magnetic meridional line declines to terminator line in these regions. In these regions, conjugate sunrise time is ahead of local sunrise time. The distributions of the sunrise time in June (Figure 2b) and December solstice (Figure 2c) also can be explained by the angle between terminator and magnetic meridional line. In June solstice, the largest angle is seen around -30 degrees in latitude and 150 degrees in longitude. Early local sunrise time can be seen in higher northern latitude in this season. Therefore the sunrise time becomes earlier when the conjugate point locates at higher north latitude. On the other hand, the terminator is almost parallel to magnetic meridional line around -30 degrees in latitude and 320 degrees in longitude, which leads its latest sunrise time in this region. In December solstice, the same situation arises in northern hemisphere. The earliest sunrise can be seen around 30 degrees in latitude and 320 degrees in longitude, and the latest sunrise is seen around 10 degrees in latitude 160 degrees in longitude.

Comparisons between the observed onset time of ionospheric heating and the calculated sunrise time are shown in Figure 3. Data which was obtained during Kp < 4 and Dst > -50 was used. Color shows time difference where the calculated sunrise time is subtracted from the observed onset time. Black line shows magnetic equator. Averages of F10.7 intensity were 202.92, 172.39, 193.25 and 197.00 for March equinox (Figure 3a), June solstice (Figure 3b), September equinox (Figure 3c), and December solstice (Figure 3d), respectively. The onset is occurred by photoelectrons which are produced just below 600 km heat local sunlit ionosphere and photoelectrons arriving from sunlit ionosphere heat predawn ionosphere. The observed onset times are almost constant (0.2 hr ahead of the calculated sunrise time) near magnetic equator in all season except June solstice. The time differences near equator in June are about 0.4 hr. This difference comes from difference of F10.7 intensity as we will discuss later. The observed onset times tend to delay in high latitude. In March equinox, late onset times which are over 1 hour behind of the calculated sunrise time were observed around -25 degrees in latitude and 360 degrees in longitude. On the other hand, early onset times which are 0.5 hour earlier than the calculated sunrise time were observed in the same region. This difference arises from origin of photoelectrons which heat ionosphere, that is, local or conjugate photoelectron heat ionosphere. The onset time of ionospheric heating by conjugate photoelectrons is usually later than that by local photoelectrons. The same situations arise in other seasons. In June solstice, late onset times were observed from -20 to -32 degrees in latitude and from 300 to 80 degrees in longitude. The latest onset time is 1.18 behind of the calculated sunrise time at -28.4 degrees in latitude and 5.2 degrees in longitude. In December solstice, late onset times were observed around 30 degrees in latitude and 180 degrees in longitude similarly. The latest sunrise (0.89 hour behind of the calculated sunrise time) is seen at 31 degrees in

latitude and 183 degrees in longitude.

We studied a relationship between the magnetic field line length and the time difference between the observed onset time and the calculated sunrise time at predawn ionosphere as shown in Figure 4. Large black dots show mean value and error bars show standard deviation. The observed onset times in both sunlit and predawn ionosphere were included in Figure 3 but the observed onset times in predawn were only used henceforth. Magnetic field line length is defined as length from 100 km altitude in sunlit ionosphere to observed height (600 km altitude) in predawn ionosphere. The observed onset times are about 10 minutes earlier than the calculated sunrise time at 100 km altitude when the magnetic field line is less than 5000 km. The time difference of 10 minutes ahead of the calculated sunrise time is corresponding to SZA of 102.3 degrees. On the other hand, the observed onset times delay and scatter as the magnetic field line length is long. Finally, the time difference become about 30 minutes behind of the calculated sunrise time when the magnetic field line length is over 10000 km. The time difference is correspond to SZA in sunlit ionosphere when the onset is observed. Maximum height of the magnetic field line is about 1200 km when the magnetic field line length is 5000 km. More than half length of the magnetic field passes through plasmasphere and exosphere. Plasmasphere and exosphere are variable. This is the reason why the time difference between observed onset time and the calculated ionospheric sunrise time fluctuate.

We found that the observed onset time varies with F10.7 intensity. Figure 5 shows F10.7 variation of the observed onset time. In the case that the magnetic field length is less than 5000 km, where the magnetic field length dependency cannot be clearly seen, the observed onset times become early as F10.7 intensity increase when F10.7 intensity is below 200 (Figure 5a). The observed onset time is almost equal to the sunrise time when F10.7 is 130. The observed onset time takes the earliest value, 22 minutes ahead of the calculated sunrise time when F10.7 is 210. When F10.7 is larger than 210, the time difference is constant or slightly late as increasing F10.7. The time difference is about 9 minutes ahead of the calculated sunrise time when F10.7 is 290. When the magnetic field line length is between 5000 and 10^4 km, similar feature still can be seen, but the standard deviations are large (Figure 5b). When the magnetic field line length is longer than 10^4 km, the time difference takes minimum value around F10.7 = 200, and then increase again (Figures 5c and 5d). The standard deviations are large because effect of the magnetic field line length variation is stronger than that of F10.7. The peak value and altitude of photoelectron production rate increases with increasing the intensity of F10.7 [Carlson and Weill, 1967]. As well known, EUV dependency on daily F10.7 change near F10.7 = 200 [cf. Richards et al., 1994]. Similar effect also can be seen in our result.

Figure 6 shows heating rate (dTe/dLT) of predawn ionosphere corresponding to the magnetic field line length. When the magnetic field line length is longer than 5000 km, average of heating rates are almost constant, about 8 K/min. These values are slightly larger than observations of 300 km altitude obtained by backscatter radar at Arecibo (4 K/min) [Carlson, 1966] and Millstone Hill (1 K/min) [Evans 1967b]. When the magnetic field line length is shorter than 5000 km, the heating rates have large variation whose maximum is over 70 K/min and minimum is about 5 K/min. The average of heating rate is 34.0 K/min when the magnetic field line length is 2000 km. When the magnetic field line length is longer than 5000 km, two different slopes are usually observed; one of them is caused by conjugate photoelectrons and another is caused by local photoelectrons. In the case that the magnetic field line length is shorter than 5000 km, there are cases that two gradient changes of heating rate could not be observed. The short magnetic field length means that sunlit foot point of magnetic field is close to predawn foot point of magnetic field. Therefore this result has prospect of containing effect of photoelectrons produced in local ionosphere.

Figure 7 shows heating rate associated with SZA in sunlit ionosphere. Clear signature cannot be seen due to high fluctuation when the magnetic field length is less than 5000 km (Figure 7a). The heating rate reduce when SZA is larger than 110. On the other hand, when the magnetic field length is longer than 5000 km, the heating rates are almost constant (about 9 K/min) in SZA below 110 degrees (Figure 7b). The heating rate reduce with increasing SZA in sunlit ionosphere in the case that SZA is larger than 105 degrees. Averages of heating rate are about 7.4 K/min in 107.5 degrees and 4.3 K/min in 112.5 degrees, respectively. Small SZA in sunlit ionosphere does not represent high heating rate directly.

Discussion

When angle between magnetic meridian and terminator is large, one side of ionosphere which connected by magnetic field is sunlit and the other side of that is still dark. Above 300 km, mean free path of photoelectron is almost equal to scale height of plasma. Therefore photoelectrons can escape from sunlit ionosphere along the magnetic field line [Hanson, 1963]. Under this condition, photoelectrons arriving from sunlit ionosphere act as heat source of predawn ionosphere. Velocity of photoelectron with 10 eV is about 1.3×10^3 km/sec. Therefore photoelectron can arrive at conjugate ionosphere in a few second. The photoelectrons arriving at conjugate predawn ionosphere heat ambient plasma through Coulomb collision. The energy loss rate of photoelectron per traveling length is proportional to ambient Ne and inverse proportion to its energy [Mantas, 1975]. Large energy loss of photoelectron occurs below 300 km altitude. Especially, below 250 km altitude, electron

temperature is maintained by photoelectron heating [Roble, 1975]. In addition, this interaction between high-energy photoelectron and thermal electron is well known as the heat source of plasmasphere [Mantas et al., 1978; Rao and Maier, 1970]. Roble [1975] calculated Te variation with two cases; one case is Te variation with photoelectron heating and heat flux from plasmasphere, and another case is Te variation with photoelectron heating only. Comparing these two results, Te variations between minimum Te in night and the peak value in morning overshoot are about 1400 K in the both cases. This result shows that heat flux from plasmasphere plays an important role for maintenance of Te in the nightside and heat source of afternoon overshoot [Schunk and Nagy, 1978], but is not significant in morning overshoot of Te. Pitch angle of photoelectron vary with angle which is between direction of incident photon and magnetic field. Therefore the pitch angle has local time and seasonal variation. But the pitch angle variation is not important in the morning because the angle between direction of incident photon and magnetic field is almost 90 degrees [Mariani, 1964].

The onset of ionospheric heating is observed when energy production by photoelectron exceeds heat conduction and energy losses to ion and neutral species. The onset time indicate flux of photoelectron escaping from sunlit ionosphere. The escaping flux increases as the onset delay because the production rate of photoelectron exponentially increases as the onset delay, in other word, SZA becomes smaller [Carlson and Weill, 1967].

When SZA becomes 102 degrees, the onsets are observed at where the magnetic field line is shorter than 5000 km. SZA in sunlit ionosphere is constant irrespectively of the magnetic field line length and the heating rate of electron increases with decreasing the magnetic field line length. The flux of photoelectron escaping from sunlit ionosphere increases exponentially around SZA of 102 degrees. Large flux arrives at predawn ionosphere abruptly and this flux acts as large heat source which greatly exceeds the heat conduction and the energy losses when the magnetic field line length is shorter than 5000 km. The flux which exceeds the heat conduction and the energy losses can be observed as the heating rate.

On the other hand, when the magnetic field line length is longer than 5000 km, SZA in sunlit ionosphere decreases as the magnetic field line length becomes longer. Heating rate of electron is almost constant irrespective of the magnetic field line length. In this case, the flux produced at SZA of 102 degrees is unsatisfactory to heat up predawn ionosphere. The flux produced at sunlit ionosphere increases as SZA decreases. Therefore small SZA which can produce large flux is required when the magnetic field is long. The flux arriving at predawn ionosphere increases gradually as SZA becomes smaller. The heating rate is the energy production by photoelectrons which exceeds the heat conduction and the energy

losses. Because the heating rate is observed as soon as the energy production exceeds the energy losses, constant heating rate is only observed.

Our results suggest that larger flux of photoelectron escaping from sunlit ionosphere is required to heat up predawn ionosphere as the magnetic field line becomes longer. If we assume that the same flux is required as predawn heating, our result show that larger flux escaping from sunlit ionosphere is required as the magnetic field line becomes longer. Namely, the flux of photoelectron decrease during traveling from sunlit to predawn ionosphere due to trapping in plasmasphere, Coulomb collision with ambient plasma, elastic and inelastic collision with neutral atmosphere.

Production rate of photoelectron also vary with intensity of solar activity F10.7. Enhancement of F10.7 intensity has the same effect as reduction of SZA. Therefore SZA in sunlit ionosphere decreases with increasing F10.7. Thermosphere also expands as F10.7 increase. As the result, collision with neutral species increases. When F10.7 is stronger than 200, expanding effect overtake effect of the flux enhancement. Therefore the onset delays with increasing F10.7. This effect is pronounced when the magnetic field length is long.

Summary

We studied distribution of the observed onset time of ionospheric heating in low- and mid-latitude by using data of HINOTORI satellite. First finding is that the observed onset times of ionospheric heating vary with the magnetic field line length and F10.7. The onset occurs between sunlit SZA of 90 and 110 degrees. Second finding is that the heating rate of electron temperature decrease with the magnetic field line length increase. Just after sunrise, heating rate of ionosphere is equal to energy production by photoelectrons, which is proportional to arriving flux of photoelectron [Evans, 1967b], but this energy balance break down soon because energy loss by collisions with ion and neutral species and heat conduction become important [Bauer et al., 1970]. Therefore our results of heating rate do not show energy production by photoelectrons arriving from conjugate directly. Photoelectron plays an important role for heat source of plasmasphere in early morning because large flux loss is suggested from our results. Simultaneous observations of Te profile, ion and neutral temperature are necessary to study the energy balance at the beginning of morning overshoot. At the same time, detail calculations of electron ion temperature help us understand energy balance of predawn ionosphere.

References

Balan, N., K.-I. Oyama, G. J. Bailey, and T. Abe (1996), Plasmasphere electron temperature profiles and effects of photoelectron trapping and an equatorial high-altitude heat source, J.

Geophys. Res., 101, 21, 689-21,696.

Barbier, D. (1961), Les variations d'intensite de la raie 6300 Å de la luminescence nocturne, *Ann. Geophys*., 17, 3-15.

Bauer, P. G., and M. Petit (1970), Thermal coupling between the upper F2-region and magnetosphere: Heat fluxes and energy production, Planet. Space Sci., 18, 1447-1470.

Chao, C. K., S.-Y. Su, and H. C. Yeh (2003), Presunrise ion temperature enhancement observed at 600 km low- and mid-latitude ionosphere, *Geophys. Res. Lett*., 30, 1187, doi:10.1029/2002GL016268.

Carlson, H. C. (1966), Ionospheric heating by magnetic conjugate-point photoelectrons, *J. Geophys. Res.*, 71, 195-199.

Carlson, H. C., and G. M. Weill (1967), Solar cycle variation of conjugate photoelectron flux onset timing deduced from 6300 Å and Te observations, *Ann. Geophys*., vol 23, 569-572.

Carlson, H. C. (1968), Most recent studies of low latitude effects due to conjugate location heating, Radio Sci., 3, 668-673.

Cole, K. D. (1965), The predawn enhancement of 6300 Å airglow, *Ann. Geophys*., 21, 156-158.

Evans, J. V. (1967a), Midlatitude F-region densities and temperature at sunspot minimum, *Planet. Space Sci.*, 15, 1,387-1,405.

Evans, J. V. (1967b), Midlatitude electron and ion temperatures at sunspot minimum, *Planet. Space Sci.*, 15, 1,557-1,570.

Hanson, W. B. (1963), Electron temperatures in the upper atmosphere, *Space Res*., 3, 282.

MacPherson, B., S. A. Gonzalez, M. P. Sulzer, G. J. Bailey, F. Djuth, and P. Rodriguez (2000), *J. Geophys. Res.*, 105, 23,055-23,067.

Mantas, G. P. (1975), Theory of photoelectron thermalization and transport in the ionosphere,

Planet. Space Sci., 23, 337-354.

Mantas, G. P., H. C. Carlson, and V. B. Wickwar (1978), Photoelectron flux buildup in the plasmasphere, *J. Geophys. Res.*, 81, 1-15.

Mariani, F. (1964), Pitch-angle distribution of the photoelectron and origin of the geomagnetic anomaly in F2 layer, J. Geophys. Res. 69, 556-560.

Nagy, A. F., and P. M. Banks (1970), Photoelectron fluxes in the ionosphere, *J. Geophys. Res.*, 31, 6,260-6,270.

Oya, H., T. Takahashi and S. Watanabe (1986), Observation of low latitude ionosphere by the impedance probe on board the Hinotori satellite, *J. Geomag. Geoelectr.*, 38, 111-123.

Oyama, K.-I., K. Schlegel, and. S. Watanabe (1988), Temperature structure of plasma bubbles in the low latitude ionosphere around 600 km altitude, *Planet. Space Sci.*, 36, 553-567.

Oyama, K.-I. (1994), Verification of IRI plasma temperature at great altitude by satellite data, *Adv. Space Res*., 14(12), 105-113.

Oyama, K.-I., S. Watanabe, Y. Su, T. Takahashi, and K. Hirao (1996), Season, local time, and longitude variation of electron temperature at the hight of ~600 km in the low latitude region, Adv. Space Res., 18(6), 269-278.

Rao, B. C. N., and J. L. Donley (1969), Photoelectron flux in the topside ionosphere measured by retarding potential analyzers, *J. Geophys. Res*., 74, 1715-1719.

Rao, B. C., and E. J. R. Maier (1970), Photoelectron flux and photonospheric heating during the conjugate point sunrise, *J. Geophys. Res.*, 75, 816-822.

Richards, P. G., J. A. Fennelly, D. G. Torr (1994), EUVAC: A solar EUV flux model for aeronomic calculations, *J. Geophys. Res.*, **99**, 8,981-8,992.

Roble, R. G. (1975), The calculated and observed diurnal variation of the ionosphere over Millstone Hill, *Planet. Space Sci.*, 23, 1017-1033.

Sheperd, G. G., J. F. Pieau, T. Ogawa, T. Tohmatsu, K. Oyama, Y. Watanabe (1978), Direct measurement of conjugate photoelectrons and predawn 630 nm airglow, *Planet. Space Sci.*, 26, 211-217.

Swider, W. (1964), The determination of the optical depth at large solar zenith distances, *Planet. Space Sci.,* 12, 761-782.

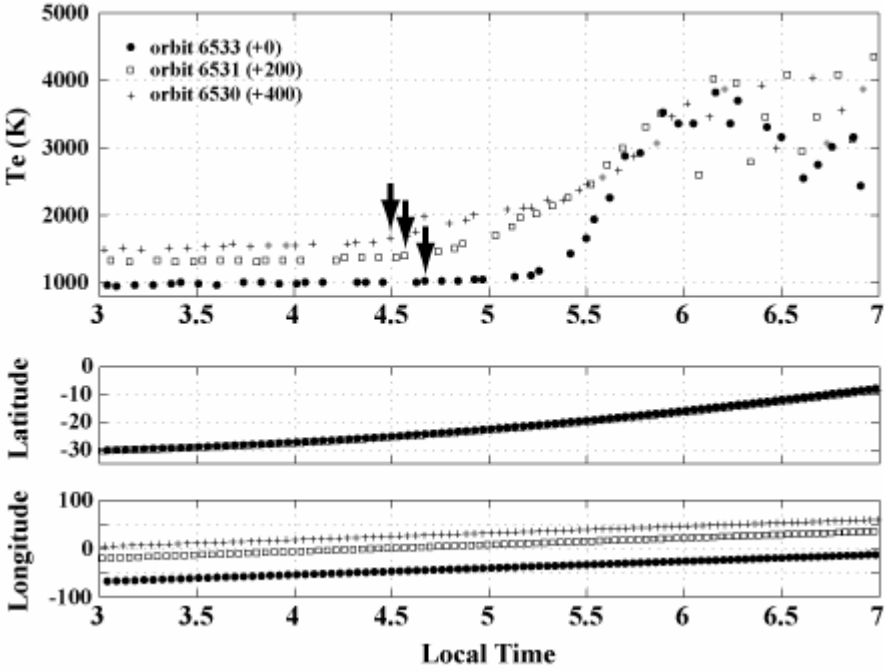

Fig. 1. Local time (LT) variations of Te (top) with respect to the satellite location of latitude (middle) and longitude (bottom) in June solstice. Electron temperatures are shifted by +200 for orbit 6531 and +400 for orbit 6530, respectively. Black arrows show onset times of ionospheric heating in each orbit.

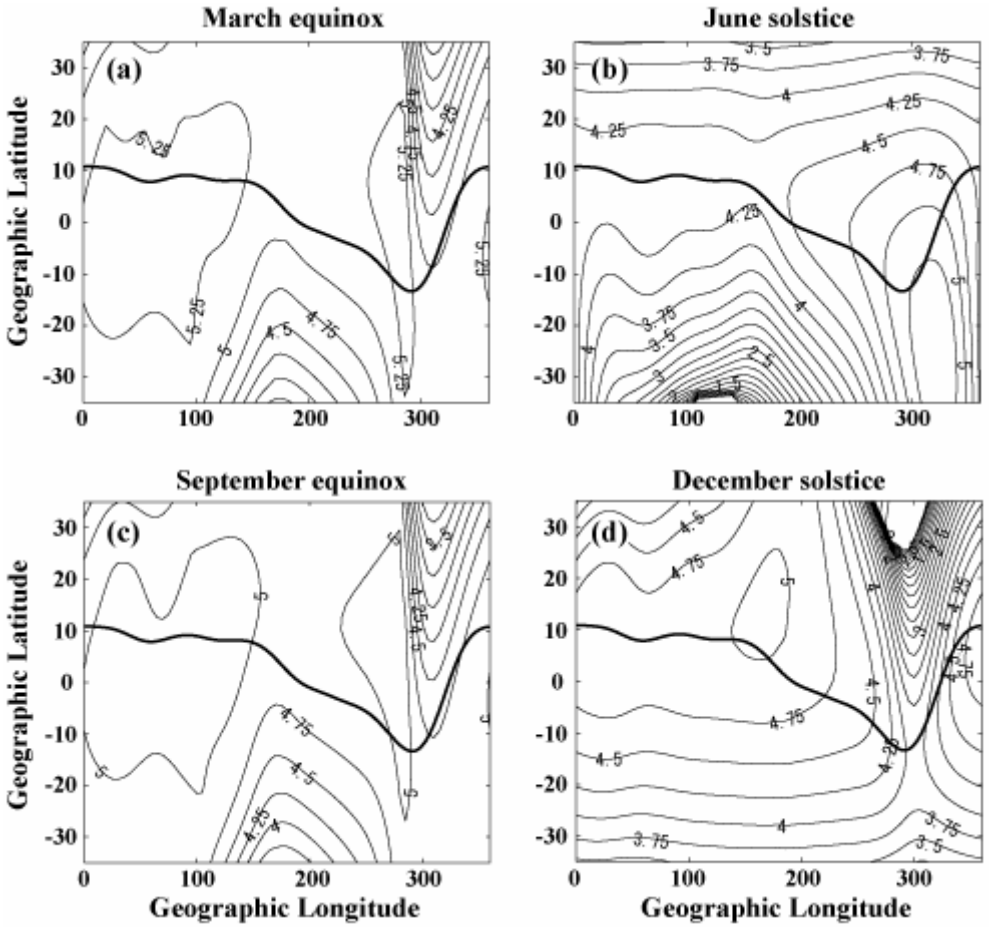

Fig. 2. Distributions of sunrise time at 100 km altitude projected to 600 km altitude in March equinox (a), June solstice (b), September equinox (c) and December solstice (d). Black thick line shows magnetic equator. Contour level is 15 minutes.

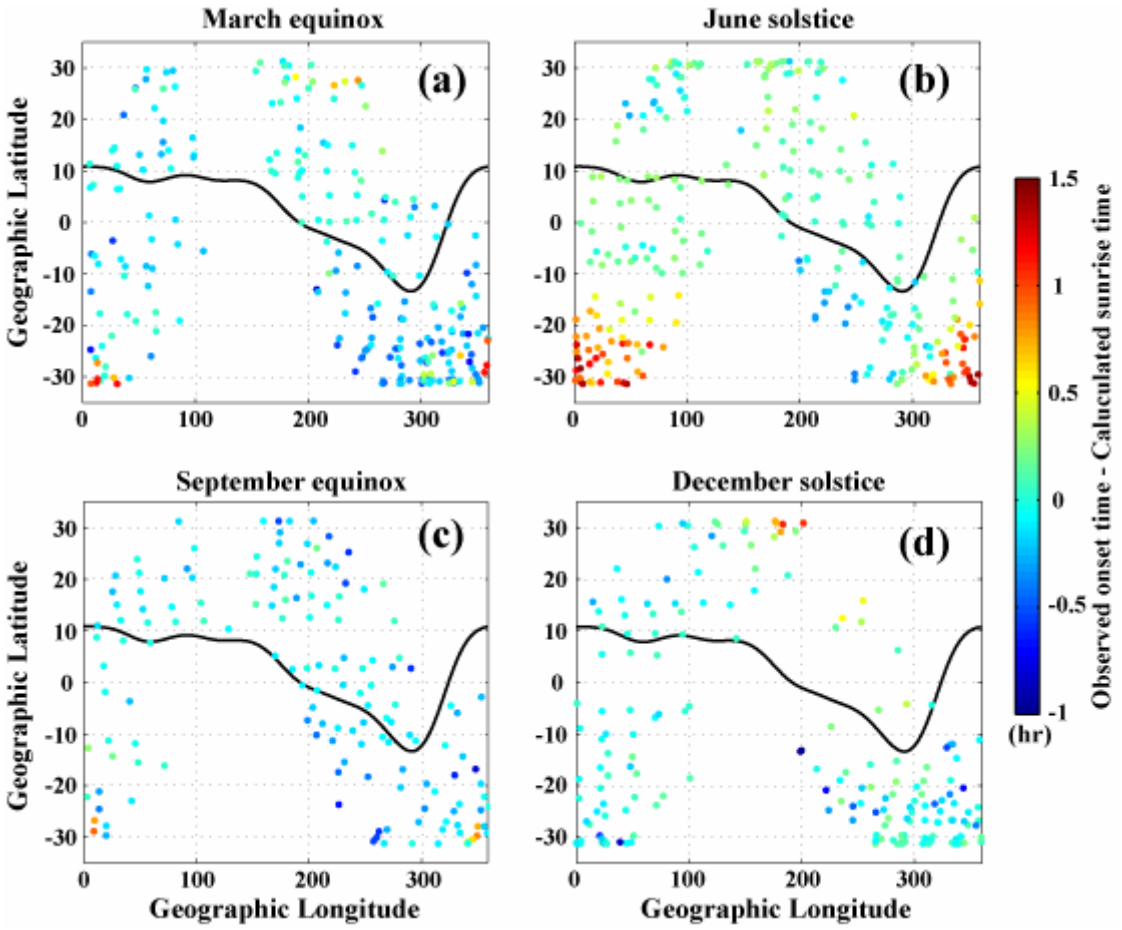

Fig. 3. Distributions of time difference between observed onset time of ionospheric heating and calculated sunrise time in March equinox (a), June solstice (b), September equinox (c) and December solstice (d). Color shows time difference between observed onset time of ionospheric heating and calculated ionospheric sunrise time. Black line shows magnetic equator.

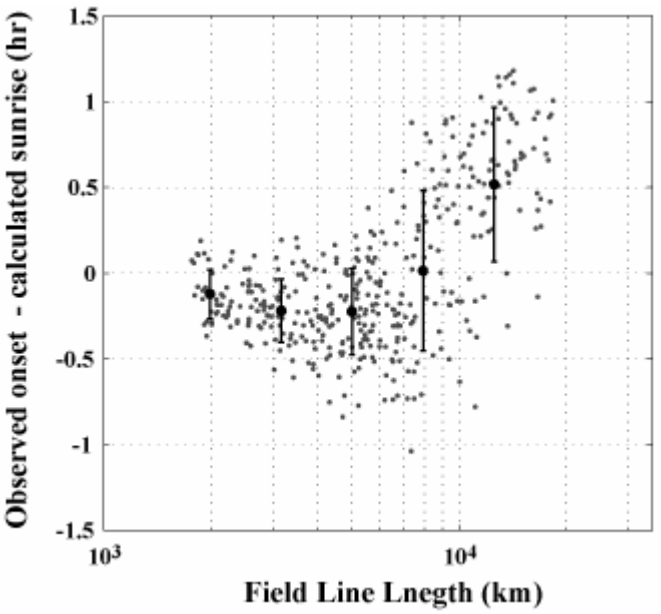

Fig. 4. Dependency of the time difference between sunrise time and observed onset time in inclination angle of magnetic field. Large black dots show mean value and error bars show standard deviation.

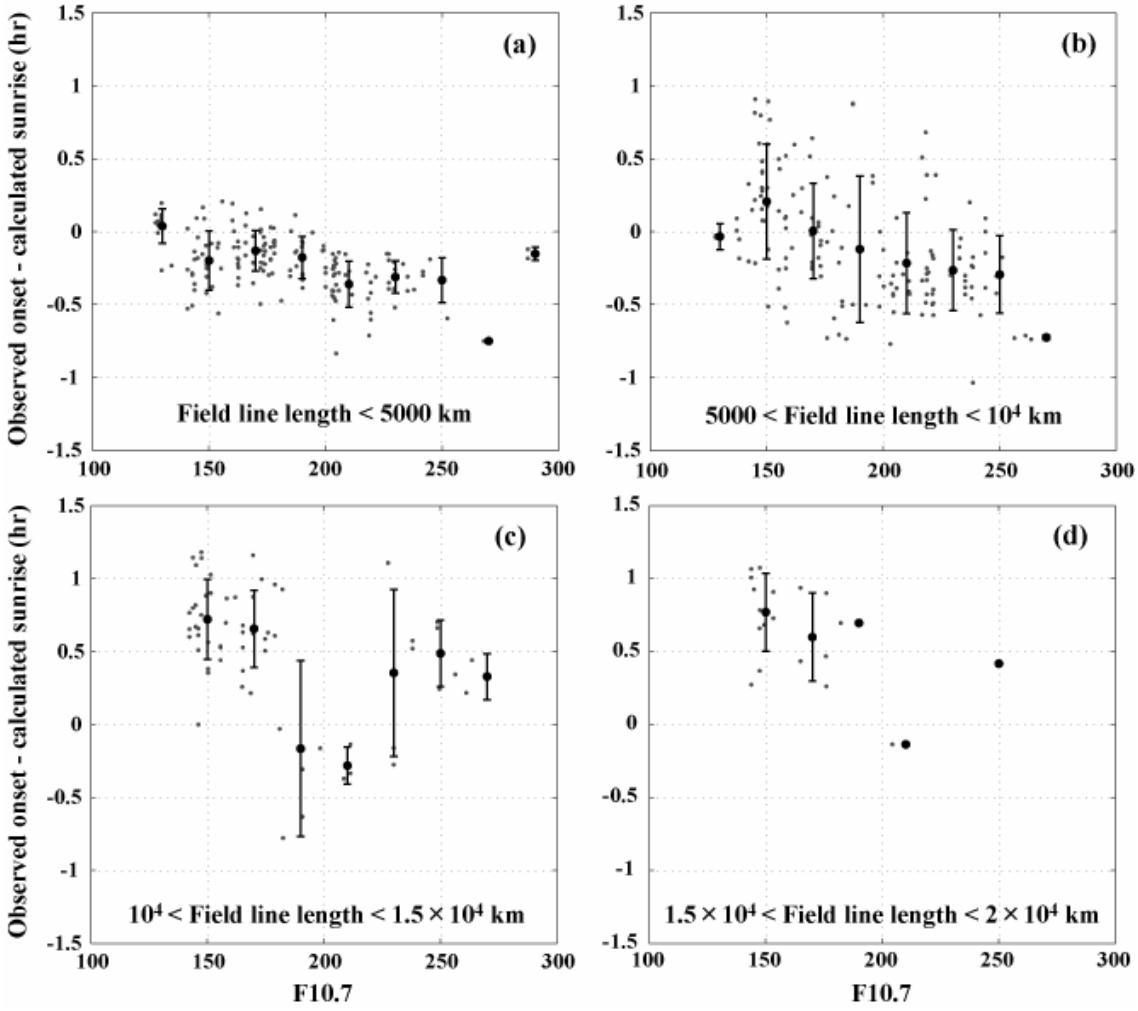

Fig. 5. The time difference between sunrise time and observed onset time in F10.7 variation when the magnetic field line is shorter than 5000 km (a) and longer than 5000 km (b). The onset time ahead as F10.7 increase when F10.7 is below 200. Large black dots show mean value and error bars show standard deviation.

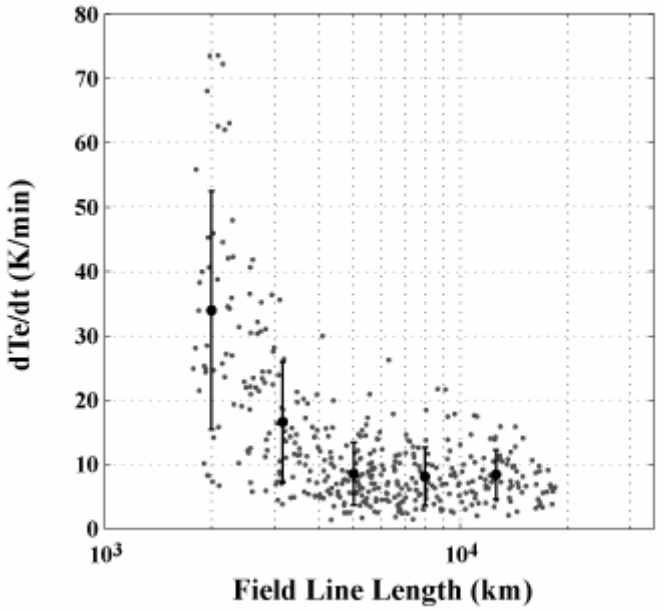

Fig. 6. Heating rate of electron temperature variation with the magnetic field line length. Large black dots show mean value and error bars show standard deviation.

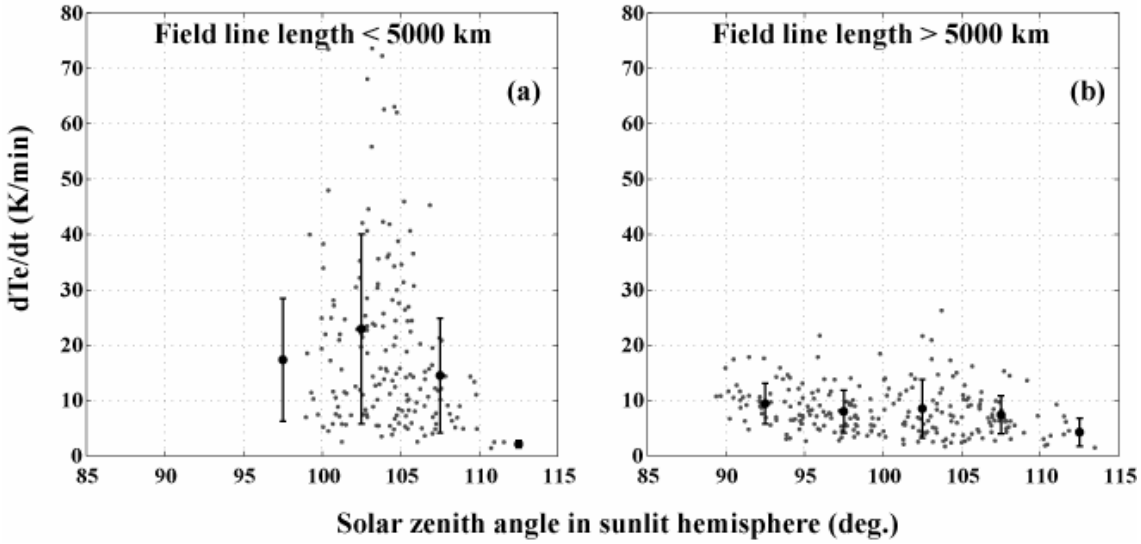

Fig. 7 Ionospheric heating rate variation with solar zenith angle in sunlit ionosphere when the magnetic field line length is less than 5000 km (a) and longer than 5000 km (b). Large black dots show mean value and error bars show standard deviation.